NASA TECHNICAL MEMORANDUM

NASA TM X-73546

NASA TM X-73546

PERFORMANCE CORRELATIONS OF FIVE SOLAR COLLECTORS TESTED SIMULTANEOUSLY OUTDOORS

by Dean R. Miller
Lewis Research Center
Cleveland, Ohio 44135

TECHNICAL PAPER presented at the
Joint Conference of the International Solar Energy
Society and the Solar Energy Society of Canada
Winnipeg, Canada, August 15-20, 1976

(NASA-TM-X-73546) PERFORMANCE CORRELATIONS OF FIVE SOLAR COLLECTORS TESTED SIMULTANEOUSLY OUTDOORS (NASA) 26 p HC A03/MF A01 CSCL 10A

N77-15487

Unclas
G3/44 11458

PERFORMANCE CORRELATIONS OF FIVE SOLAR COLLECTORS TESTED SIMULTANEOUSLY OUTDOORS

by Dean R. Miller

Lewis Research Center

E-8982

ABSTRACT

Collector thermal efficiency, and efficiency degradation with time were measured for 5 flat-plate solar collectors tested simultaneously in an outdoor solar collector test facility.

Results indicate that by using collector performance parameters which account for diffuse insolation, outdoor data recorded on "cloudy" days can be used as a measure of performance, as long as the ratio of direct to total insolation exceeds approximately 0.6. These outdoor results also show good agreement with thermal efficiency data obtained indoors in a solar simulator.

Significant efficiency degradation occurred on only one of the five collectors exposed to outdoor conditions for a period of one to two years.

STAR Category 44

INTRODUCTION

A major problem associated with the evaluation of solar collector performance obtained outdoors, has been the necessity to record data only on clear days. Since it is possible to collect a significant amount of energy on a day with scattered clouds, the need to evaluate collector performance on such a "cloudy" day has long been recognized.

Recently, a correlation technique was reported (ref. 1) in which diffuse insolation, as well as time variations of direct and diffuse insolation, was taken into account. This approach separates those solar variables which affect collector thermal efficiency (e.g., flux, incident angle, etc.), from parameters that are a unique part of a collector design (e.g., absorbtance, transmittance, heat loss, etc.). By using this analytical technique, it is possible to measure collector efficiency using data obtained on both clear and cloudy days, in an outdoor test facility. This report describes those tests and discusses the results obtained.

Collector thermal efficiency and efficiency degradation with time were measured for five flat-plate solar collectors tested simultaneously in an outdoor test facility. Data were analyzed using both the analysis presented in reference 1, as well as by comparison with baseline data measured under indoor, simulated sun conditions.

EXPERIMENTAL APPARATUS

The outdoor solar collector test facility is shown in figure 1. The test facility consists of two collector test stands, each with the capability to simultaneously test five flat-plate solar collectors. The mechanical components of the flow loop (pump, water tank, etc.) are enclosed in the instrument shed which is located in the center of each stand.

Coolant Flow Loop

The liquid used as a coolant is a 50-50 mixture, by weight, of ethylene glycol and water. Corrosion inhibitors are present in the ethylene glycol (ref. 2).

Figure 2 shows a schematic of the flow loop of one of the collector test stands. Note that each collector has an independent flow loop which is in parallel with the other four collector flow loops. An expansion tank is provided to allow for changes in fluid volume.

The coolant is circulated by a 1/4 hp pump, with a surge tank connected at it's outlet. Coolant is stored in a commercially available 80-gallon water tank which has two 5500-watt immersion heaters. In general, the tank heaters are used to maintain a constant storage temperature.

The air liquid heat exchanger is used to regulate the inlet temperature to the collectors. In the event that the inlet manifold temperature increases above the "set" temperature, an automatic controller operates a series of valves which route the hot fluid to the heat exchanger, where the excess heat is dumped.

Flow control for each individual collector is achieved by the adjustment of a remotely-operated valve. Also, since a constant pressure is required in the collector inlet manifold, a collector bypass line is provided.

For those collectors with aluminum absorber plates, an aluminum screen is placed in the flow path just upstream of the inlet to the collector.

Filtration of the water-glycol mixture is provided by a 25 micron filter, located just downstream of the pump.

INSTRUMENTATION

The following measurements are recorded for each collector:

(1) Coolant flowrate

(2) Coolant temperature at the inlet to the collector

(3) Coolant temperature at the outlet to the collector

(4) Absorber plate temperature

(5) Coolant pressure at inlet to the collector

(6) Pressure differential across the collector

The coolant flowrate through each collector is measured with a turbine-type flowmeter. The flowmeters were calibrated for a 50-50 mixture of ethylene glycol and water by the vendor.

In order to make a "gross" check on flowmeter output, the capability to "grab-sample" the fluid has been incorporated into the coolant flow loop. By withdrawing a sample of fluid from a collector flow loop, and knowing the time interval over which the sample was taken and the fluid temperature, it is then possible to compute the fluid flowrate. Checks of this nature are periodically performed on each flowmeter.

Collector temperatures are measured with Chromel-constantan thermocouples (ISA-TYPE E). The inlet and outlet thermocouples were made from the same spool of wire, and were calibrated in an oil bath. Then the inlet and outlet thermocouples were matched so that their combined error is within $\pm 0.5^{\circ}$ F.

A check is performed on the inlet and outlet thermocouples prior to installation of a collector on the test stand, and also after removal. This check is done by immersing both the inlet and outlet thermocouples in an ice bath and then in a boiling water bath.

Solar radiation is measured in the plane of the collectors, and in the horizontal plane. A pyranometer on each test stand is oriented at the collector tilt angle. Solar instruments located on a nearby roof are also used to measure the total insolation (horizontal surface), the diffuse insolation (horizontal surface), and the normally incident direct radiation.

Each of the four pyranometers was checked in the solar simulator (ref. 3) every six months, at a high flux of 300 Btu/hr-ft^2, and at a low flux of 100 Btu/hr-ft^2. The four pyranometer outputs are compared to each other and also to a standard pyranometer of the same brand name and type. The standard is not used outdoors; it is stored in a light tight container. The desiccant charge in each pyranometer is routinely checked, and changed if necessary.

Solar instruments in the horizontal plane are used as a check on the solar instruments in the plane of the collectors. The output of the pyranometers on each test stand are also compared to each other. Agreement within ±3 percent is typical.

In addition to the collector and insolation data, the following weather data are recorded:

(1) ambient air temperature

(2) windspeed and wind direction

(3) relative humidity

DATA ACQUISITION

The outputs of the various types of instrumentation pass through signal conditioners and then into a matrix-type patchboard. The signals are then routed to a high speed integrating voltmeter which scans each instrumentation channel and digitizes the millivolt signal for storage on magnetic tape. Sufficient capacity exists for the on-line retrieval of the millivolt outputs of each channel. Also, an on-line access to a computer allows for output in engineering units.

EXPERIMENTAL TEST PROCEDURE

Prior to outdoor tests, a carefully controlled performance test was conducted on each solar collector in a solar simulator. Upon completion of this "baseline" test, the collector was then considered for outdoor testing. The primary criteria for selection of collectors for outdoor testing were:

(a) Performance as indicated from the simulator. Does the collector have a "high" efficiency when operated at inlet fluid temperatures characteristic of solar powered air conditioning systems?

(b) Collector design. Is there a new concept involved in the collector which exhibits some special potential for advancing collector technology, especially with regard to air conditioning applications?

Once a collector was selected for outdoor testing, it was installed on one of the outdoor test stands. Data were recorded over a period of 1 to $1\frac{1}{2}$ years to:

(1) Evaluate collector efficiency degradation with time

(2) Evaluate collector durability under "real" environmental conditions (rain, wind, snow, etc.)

(3) Evaluate and compare the efficiency of various types of collectors which are operated outdoors, simultaneously

(4) Establish a complete collector performance prediction model

Efficiency degradation was then determined by correlating the data in the manner discussed in reference 1. Any changes in the slope or intercept of the performance curve ("modified" efficiency versus "modified" $\frac{T_{IN} - T_{AMB}}{\text{flux}}$ were noted. An increase in slope indicated that the heat loss had increased. A change in the intercept indicated that the product (heat removal efficiency factor times the absorbtance times the transmittance) had changed, too.

The significance of this correlative technique is that baseline collector efficiency, and degradation of efficiency with time can be determined by recording only outdoor collector test data on either clear or cloudy days.

RESULTS AND DISCUSSION

Results of simultaneous outdoor tests on five solar collectors are presented in figures 6(a) to (e), respectively. The physical features of each collector are contained in table I. The range of operating conditions (flowrate, etc.) and weather variables (solar flux, etc.) pertaining to these data are listed in the legends in figure 6. The data were averaged over a six-hour interval of time, beginning 3 hours before solar noon, which is considered representative of an all-solar day average.

Several observations can be made from the results presented in figure 6. First, data recorded on cloudy days exhibit about the same degree of scatter as data recorded on clear days. Second, the cloudy day data show the same general trends as the clear day data. These results indicate that by accounting for diffuse insolation in the collector parameters, η^* and θ^*, data recorded on cloudy days can be used as a measure of collector performance.

However, this is not always the case. The degree and type of cloudiness for which data are shown in figure 6 corresponds to a ratio, R, of direct to total insolation greater than 0.6. Other preliminary data, not included in this report, tend to show relatively large scatter whenever the ratio R is less than approximately 0.6. Hence, it appears that the use of data recorded on cloudy days should be limited to values of R greater than approximately 0.6.

Another observation that can be made by examining figures 6(a), (b), and (c) is that, in general, efficiency data recorded in the outdoor test facility (symbolled points) agrees reasonably well with the results obtained indoors in a solar simulator (solid fairing). This indicates that the corresponding collectors experienced no significant efficiency degradation during this period of exposure to actual outdoor conditions. For these tests, that period ranged from 1 to 2 years, depending on the particular collector.

The collector corresponding to figure 6(d) did exhibit consistently lower efficiency outdoors than was recorded indoors under simulated sun conditions. This difference was attributed to what appeared to be an "oily" film that built up on the inside surfaces of both glazings of the collector. A least-squares fit of the data would indicate a significantly different intercept than the simulator curve, supporting the notion of a possible change in the transmittance of the glazings.

The collector corresponding to figure 6(c) also exhibited lower efficiency outdoors than was recorded indoors, particularly at values of θ^* greater than 0.4. A least squares fit of the data, however, would result in about the same intercept as that of the simulator curve, indicating a probable change in the heat loss of the collector. The same phenomenon has been noted in previous tests of other collectors with selective coatings when operated at

much lower ambient temperatures than those corresponding to the simulator data taken at approximately 75° F.

To further illustrate this apparent effect of ambient temperature, the data of figure 6(c) are replotted for ambient temperatures above 35° F and below 35° F in figures 7(a) and (b), respectively. There is a lack of correlation with simulator results when the ambient temperature is below 35° F, particularly at higher values of θ^*. The reason or reasons for this lack of correlation is not apparent, and will require more study and information for an explanation.

Data presented in figures 6(a) through (e) are repeated in figures 8(a) through (e), respectively, although the data in figure 8 were averaged for only a single hour. Note the increased range of scatter relative to the all-day averaged performance data of figure 6. This result demonstrates that hourly averaged data are much more sensitive to changing insolation and weather conditions, and would thereby be more difficult to correlate.

Collector efficiency on a clear winter day is presented in table II and compared to that recorded on a cloudy winter day. (Strip-chart recordings of direct solar radiation are presented in fig. 9 for these days).

CONCLUSIONS

Collector efficiency, and efficiency degradation with time were measured for five flat-plate solar collectors tested simultaneously in an outdoor solar collector test facility. Data were analyzed using an analytical technique which accounts for diffuse insolation. The following major results were obtained:

(1) By using collector performance parameters which account for diffuse insolation, outdoor data recorded on both clear and "cloudy" days may be used as a measure of performance, as long as the ratio of direct to total insolation exceeds approximately 0.6.

(2) Thermal efficiency data recorded outdoors agreed reasonably well with results obtained indoors in a solar simulator. One exception was noted

when the ambient temperature associated with the outdoor data was below 35° F. Corresponding simulator data were recorded at an ambient temperature of about 75° F.

(3) Significant efficiency degradation with time outdoors occurred on only one of the five collectors tested outdoors for a period of 1 to 2 years. This degradation was attributed to what appeared to be an oily film that built up with time on the inside surfaces of both glazings of the collector.

(4) Collector efficiency data averaged for only a single hour of the solar day appear to be quite sensitive to changing insolation and weather conditions, and are thereby difficult to correlate. Averaging these same data for a six-hour period, beginning three hours before solar noon, is considered representative of an all-day solar average.

SYMBOLS

a_θ	collector performance constant, dimensionless
b_θ	collector performance constant, dimensionless
b_o	angular response constant, dimensionless
F_R	collector plate heat-removal efficiency, dimensionless
$K_{\alpha\tau}$	incident angle modifier, dimensionless
Q_{df}	incident diffuse solar radiation, Btu/hr-ft^2, in plane of collector
Q_{dr}	incident direct solar radiation, Btu/hr-ft^2, in plane of collector
Q_T	total solar radiation, Btu/hr-ft^2, in plane of collector
Q_u	useful energy collected, Btu/hr-ft^2
N	number of instantaneous data values
R	ratio of direct to total insolation, dimensionless
T_a	ambient temperature, ^oF
T_1	fluid inlet temperature, ^oF
U_L	overall collector heat loss coefficient, Btu/hr-ft^2-^oF
α	collector surface absorptance, dimensionless
η	collector efficiency, dimensionless
η^*	"corrected" collector efficiency, dimensionless
τ	effective transmittance
θ^*	"corrected" $\dfrac{T_{IN} - T_{AMB}}{Q_T}$, Hr-ft^2-$^oF$/Btu
θ_i	solar incident angle, deg

APPENDIX A

The correlative method discussed in reference 1 is used as a basis for evaluating solar collector performance indoors (under simulated sun conditions) and outdoors (under real sun conditions).

The determination of steady-state or instantaneous efficiency by the use of the simulator facility resulted, as given in reference , in the following collector performance equations:

$$\eta = a_\theta \left[K_{\alpha\tau} \frac{Q_{dr}}{Q_T} + \frac{Q_{df}}{Q_T} (1 + b_o) \right] - \frac{b_\theta (T_1 - T_a)}{Q_T} \quad (1)$$

$$K_{\alpha\tau} = 1.0 + b_o \left(\frac{1}{\cos(\theta_i)} \right) - 1 \quad (2)$$

where

$$a_\theta = F_R \cdot (\alpha \cdot \tau)_{\theta_i = 0}$$

and

$$b_\theta = F_R \cdot U_L$$

In equation (1), the coefficients a_θ and b_θ govern the amount of solar energy transmitted and absorbed, and the amount of energy (radiant and convection) lost to the environment. These two coefficients and the angular response coefficient (b_o) are the key quantities to be obtained from any collector correlation.

For a known number (N) of instantaneous weather values obtained in any interval of time (t), the average collector efficiency $(\bar{\eta})$ is defined as:

$$\bar{\eta} = \frac{\sum_{1}^{N} Q_u}{\sum_{1}^{N} Q_T} \tag{3}$$

The summation of useful energy $\left(\sum_{1}^{N} Q_u\right)$ obtained by the use of equation (1) is

$$\sum_{1}^{N} q_u = a_\theta \cdot \sum_{1}^{N} \left[K_{\alpha\tau} \cdot Q_{dr} + (1 + b_o) Q_{df}\right] - b_\theta \sum_{1}^{N} T_1 - T_A \tag{4}$$

which upon substitution into equation (3) gives

$$\bar{\eta} = \left[\frac{\sum_{1}^{N} K_{\alpha\tau} \cdot Q_{dr}}{\sum_{1}^{N} Q_T} + \frac{(1 + b_o) \sum_{1}^{N} Q_{df}}{\sum_{1}^{N} Q_T}\right] - \frac{b_\theta \sum_{1}^{N} T_1 - T_A}{\sum_{1}^{N} Q_T} \tag{5}$$

Expressing the fraction of direct solar radiation as

$$R = \frac{\sum_{1}^{N} Q_{dr}}{\sum_{1}^{N} Q_T} \tag{6}$$

the diffuse fraction as

$$\frac{\sum_{1}^{N} Q_{df}}{\sum^{N} Q_T} = 1 - \frac{\sum_{1}^{N} Q_{dr}}{\sum_{1}^{N} Q_T} = 1 - R \qquad (7)$$

the average total radiation flux for the time period in which N samples of the total flux were obtained as

$$\overline{Q_T} = \frac{1}{N} \sum_{1}^{N} Q_T \qquad (8)$$

the average temperature difference as

$$\overline{(T_1 - T_A)} = \frac{1}{N} \sum_{1}^{N} (T_1 - T_A) \qquad (9)$$

And defining an average incident angle modifier as

$$\overline{K_{\alpha\tau}} = \frac{\sum_{1}^{N} K_{\alpha\tau} \cdot Q_{dr}}{\sum_{1}^{N} Q_{dr}} \qquad (10)$$

and substituting equations (6) to (10) into equation (5) gives

$$\bar{\eta} = a_\theta \left[\overline{K_{\alpha\tau}} \cdot R + (1 + b_o)(1 - R) \right] - \frac{b_\theta \overline{(T_1 - T_A)}}{\overline{Q_T}} \tag{11}$$

Equation (11) is our general correlation equation for flat plate collector performance. It can be further reduced to the form

$$\bar{\eta}^* = a_\theta - b_\theta(\bar{\theta}^*) \tag{12}$$

where

$$\bar{\eta}^* = \frac{\bar{\eta}}{x} \tag{12a}$$

$$x = \overline{K_{\alpha\tau}} \cdot R + (1 + b_o)(1 - R) \tag{12b}$$

$$\bar{\theta}^* = \frac{\bar{\theta}}{x} \tag{12c}$$

$$\bar{\theta} = \frac{\overline{(T_1 - T_a)}}{\overline{Q_T}} \tag{12d}$$

Use of equation (12), allows us (in theory) to plot $\bar{\eta}^*$ against $\bar{\theta}^*$ and obtain the key collector parameters of a_θ and b_θ from the intercept and slope of the correlation line. For such a correlation to be properly obtained, it is assumed that conditions are such that the heat loss coefficient (U_L) is not affected very greatly by changes in ambient temperature and wind speed.

REFERENCES

1. F. F. Simon and D. R. Miller, A Generalized Correlation of Experimental Flat-Plate Collector Performance, NASA TMX-71832 (1975).

2. R. W. Vernon, Solar Collector Performance Evaluated Outdoors at NASA-Lewis Research Center, NASA TMX-71689 (1974).

3. F. F. Simon, Flat-Plate Collector Performance Evaluation with a Solar Simulator as a Basis for Collector Selection and Performance Prediction, NASA TMX-71793 (1975).

TABLE I. - COLLECTOR'S TESTED

Description	Absorber	Coating	Glazing
Lewis Research Center	Copper (tube sheet)	Black paint	2 glass
MIROMIT	Steel (tubes bonded to absorber)	Black nickel	1 glass
NASA-Honeywell[a]	Aluminum (tube sheet)	Black nickel	2 glass
General Electric	Aluminum (tube sheet)	Selective surface	2 Lexan
NASA-Honeywell with Mylar honeycomb[a]	Aluminum (tube sheet)	Black paint	2 Glass

[a]Produced under contract NAS 3-17862.

TABLE II. - SIMULTANEOUS OUTDOOR COLLECTOR EFFICIENCY COMPARISON FOR A CLEAR WINTER DAY AND A CLOUDY WINTER DAY

Collector	Clear day η^* (%)	Cloudy day η^* (%)
General Electric Selective, 2-Lexan	36.3	18.7
NASA/Honeywell Black nickel, 2-glass	36.7	15.3
NASA/Honeywell Black paint, 2-glass with mylar honeycomb	36.6	14.6
Lewis Research Center Black paint, 2-glass	31.9	7.5
MIROMIT Black nickel, 1-glass	24.4	-1.8
Ambient temperature	28° F	30° F
Inlet temperature	150° F	150° F
Total insolation	273 Btu/hr-ft^2	128 Btu/hr-ft^2
Windspeed	7 mph	7 mph
Mass flowrate	10 lb/hr ft^2	10 lb/hr ft^2
R	.85	.74

Figure 1. - Outdoor collector test facility.

E-8982

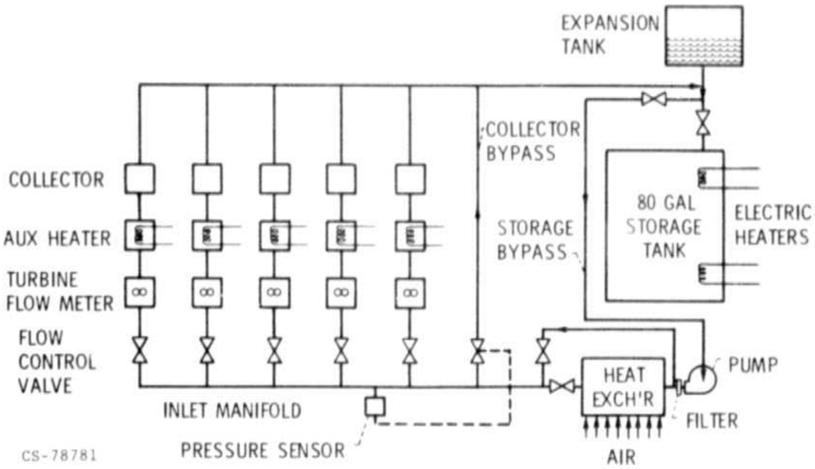

Figure 2. - Schematic of outdoor collector facility.

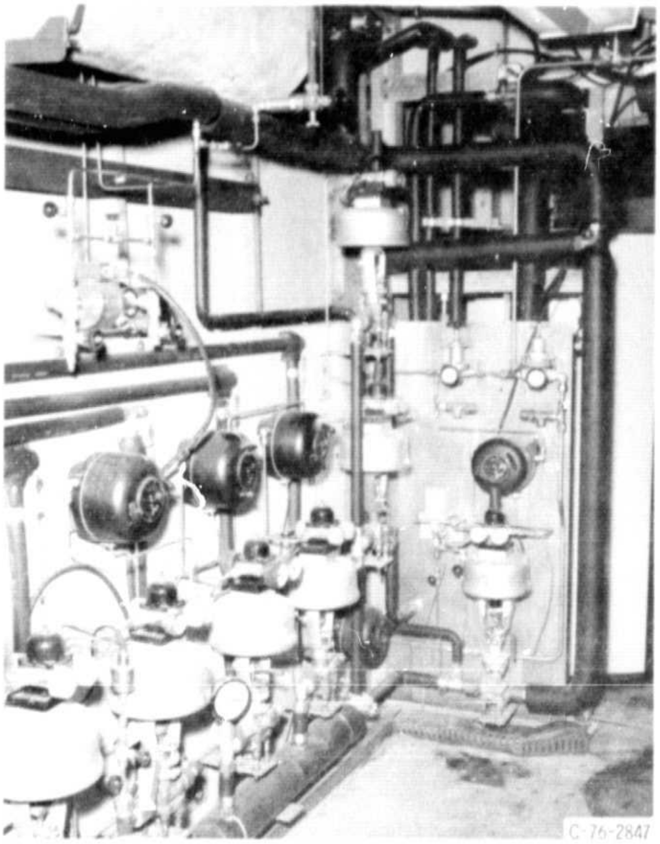

C-76-2847

Figure 3. - Coolant flow loop.

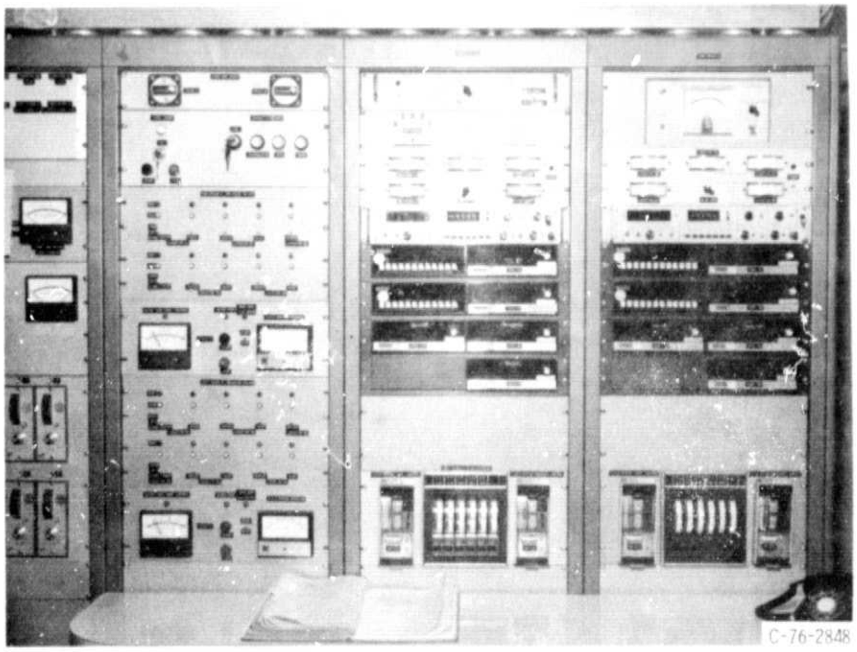

C-76-2848

Figure 4. - Control panel.

E-8982

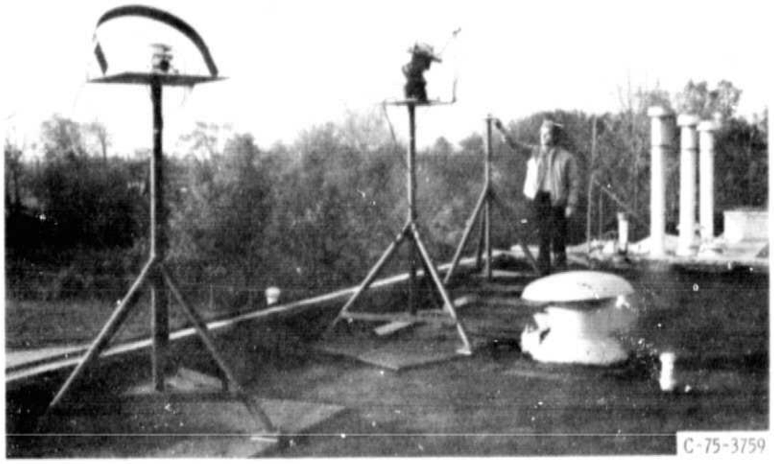

Figure 5. - Solar instruments.

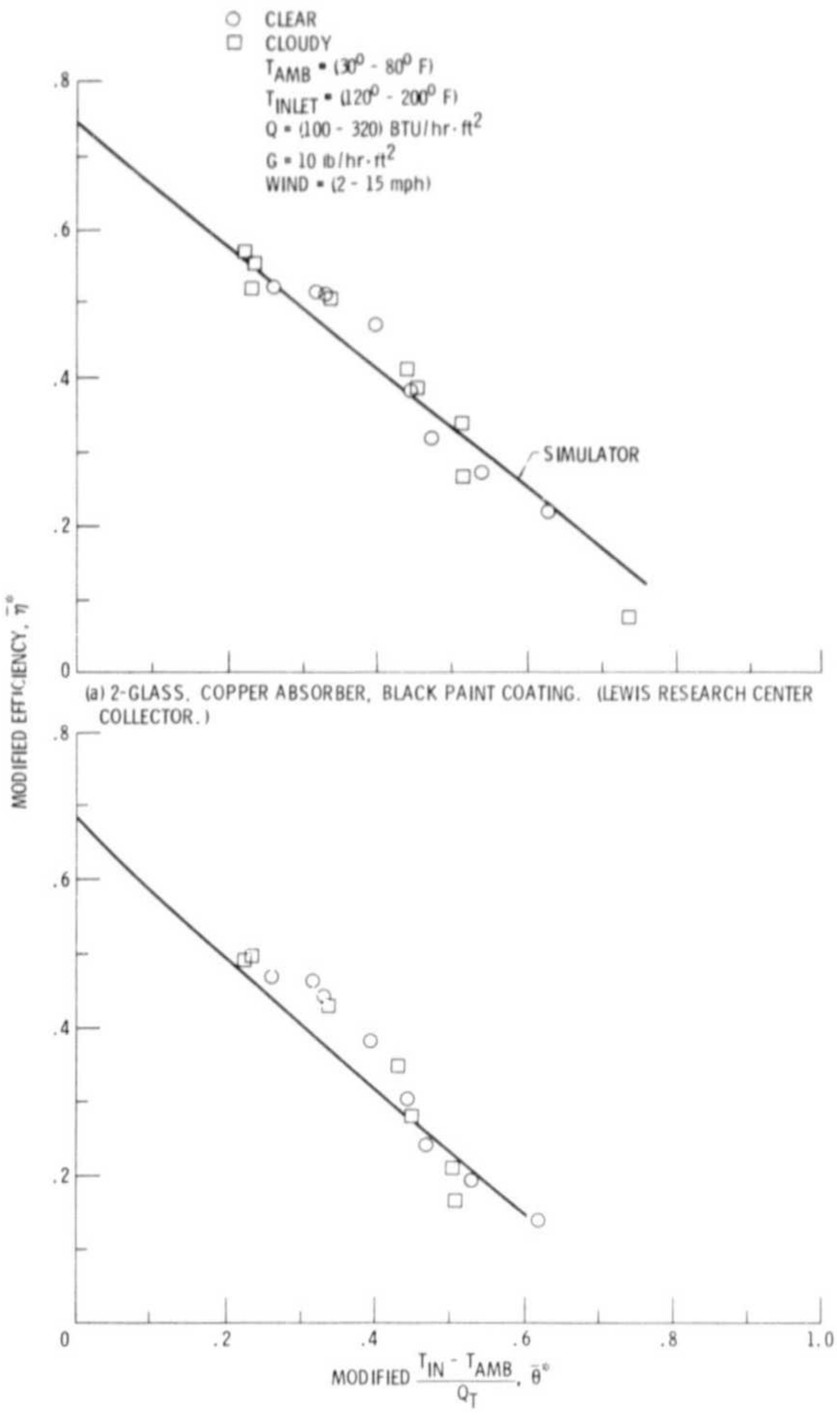

(b) 1-GLASS, STEEL ABSORBER, BLACK NICKEL COATING. (MIROMIT COLLECTOR.)

Figure 6. - All day, averaged efficiency.

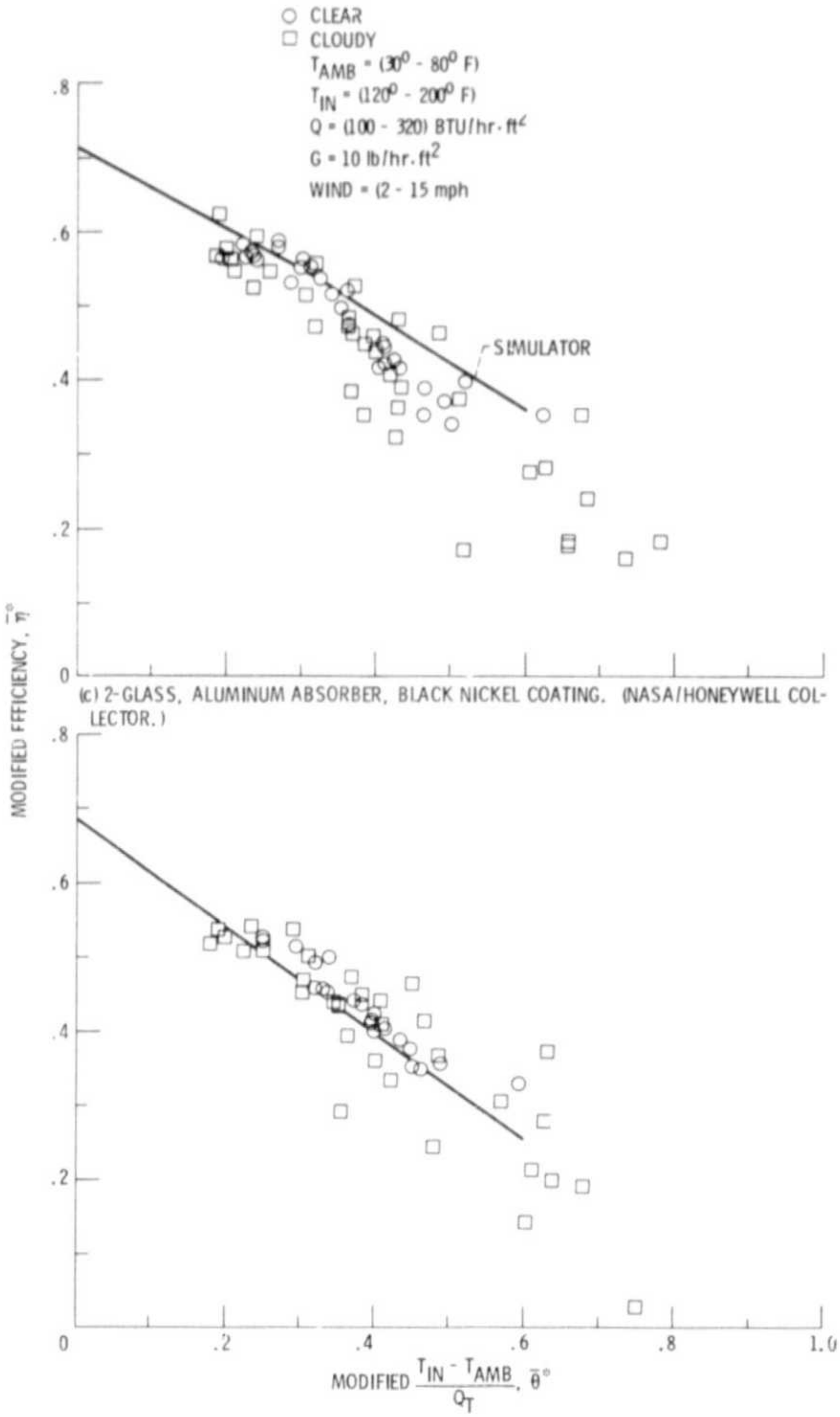

(c) 2-GLASS, ALUMINUM ABSORBER, BLACK NICKEL COATING. (NASA/HONEYWELL COLLECTOR.)

(d) 2-LEXAN, ALUMINUM ABSORBER, ALCOA ETCH COATING. (GENERAL ELECTRIC COLLECTOR.)

Figure 8. - Continued.

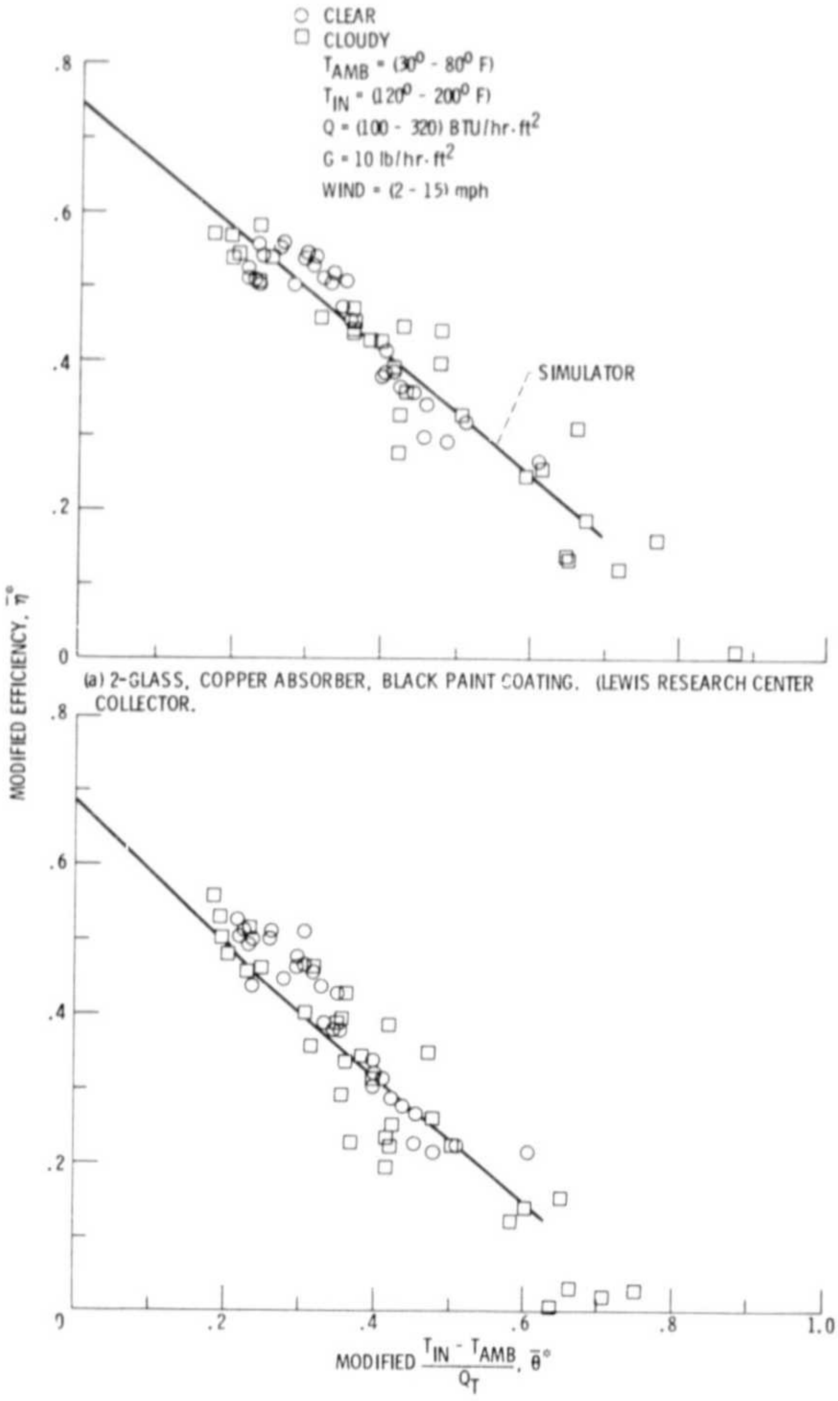

(b) 1-GLASS, STEEL ABSORBER, BLACK NICKEL COATING. (MIROMIT COLLECTOR.)

Figure 8. - Hourly averaged efficiency.

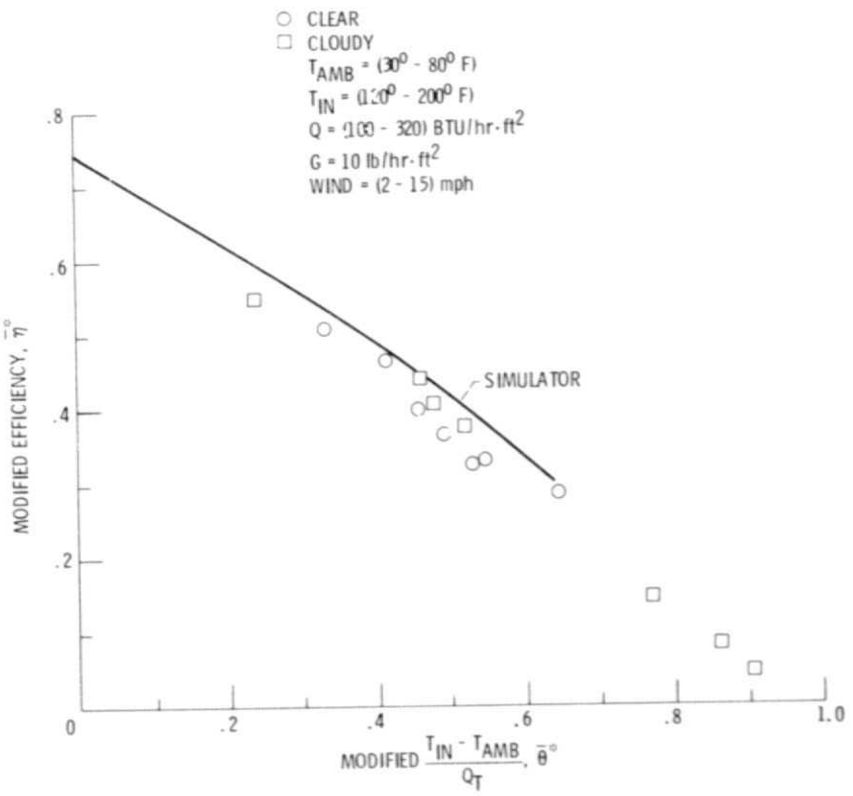

(e) 2-GLASS, ALUMINUM ABSORBER, BLACK PAINT COATING WITH MYLAR HONEYCOMB. (NASA/HONEYWELL COLLECTOR.)

Figure 6. - Concluded.

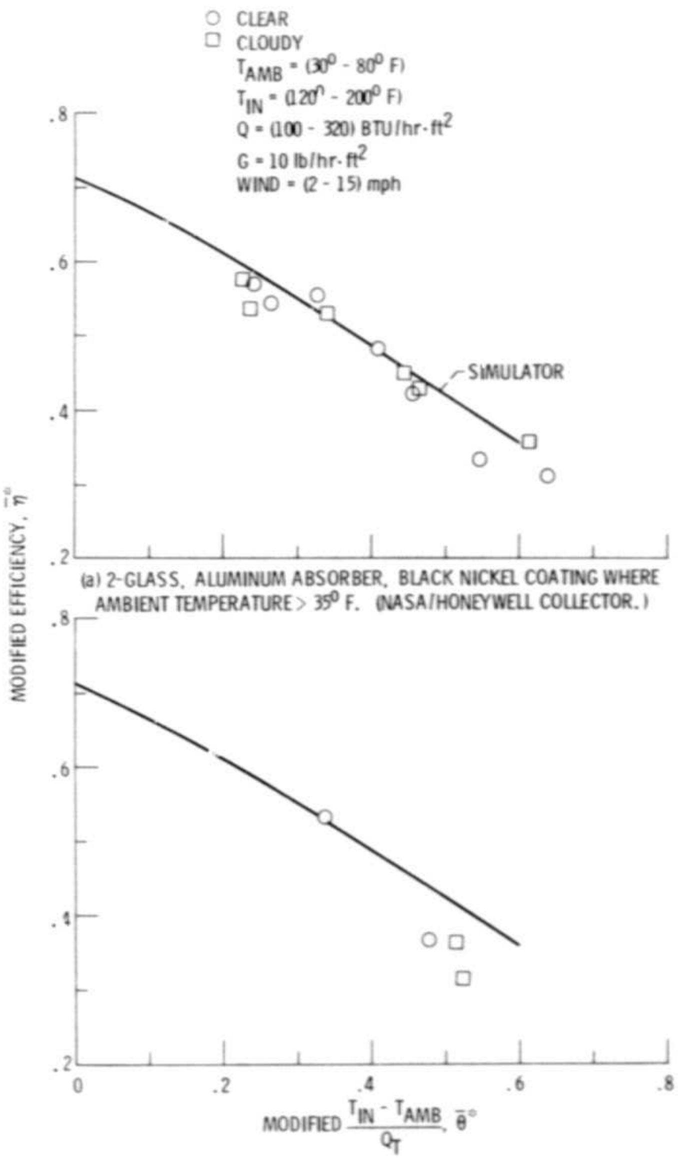

(a) 2-GLASS, ALUMINUM ABSORBER, BLACK NICKEL COATING WHERE AMBIENT TEMPERATURE > 35° F. (NASA/HONEYWELL COLLECTOR.)

(b) 2-GLASS, ALUMINUM ABSORBER, BLACK NICKEL COATING WHERE AMBIENT TEMPERATURE < 35° F. (NASA/HONEYWELL COLLECTOR.)

Figure 7. - All day, averaged efficiency.

E-8982

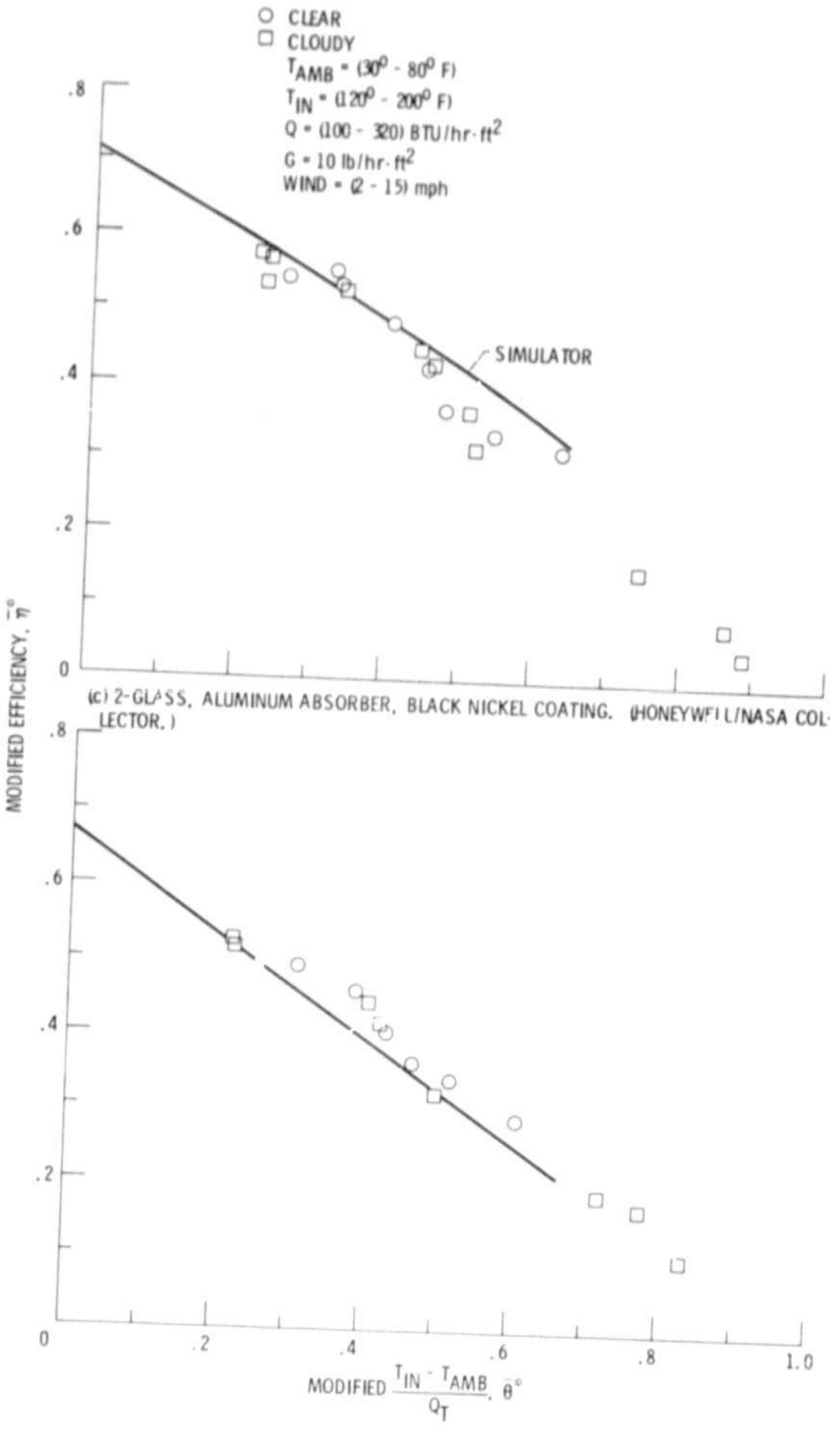

(c) 2-GLASS, ALUMINUM ABSORBER, BLACK NICKEL COATING. (HONEYWELL/NASA COLLECTOR.)

(d) 2-LEXAN, ALUMINUM ABSORBER, ALCOA ETCH COATING. (GENERAL ELECTRIC COLLECTOR.)

Figure 6. - Continued.

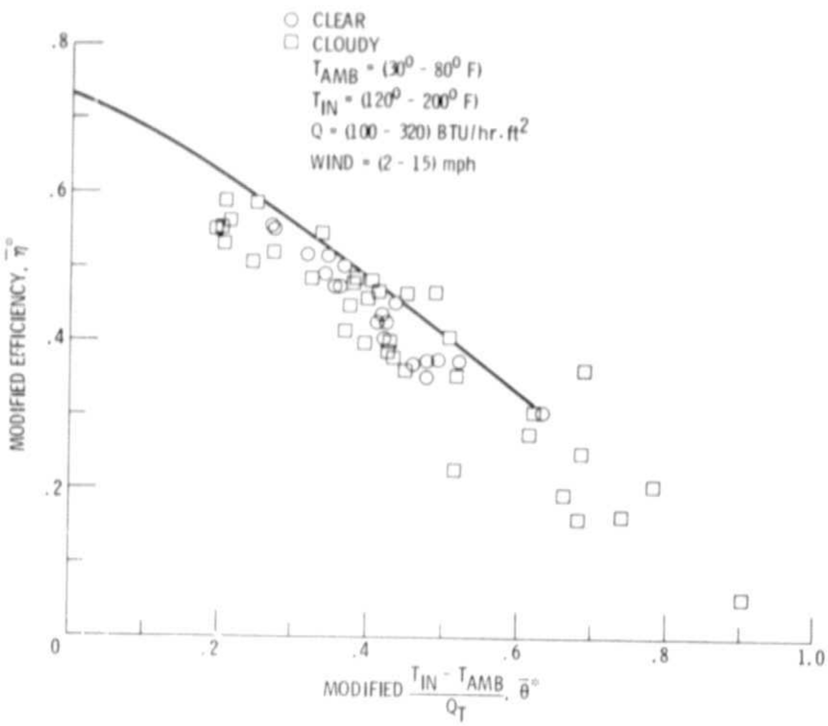

(e) 2-GLASS, ALUMINUM ABSORBER, BLACK PAINT COATING WITH MYLAR HONEYCOMB. (NASA/HONEYWELL COLLECTOR.)

Figure 8. - Concluded.

E-8982

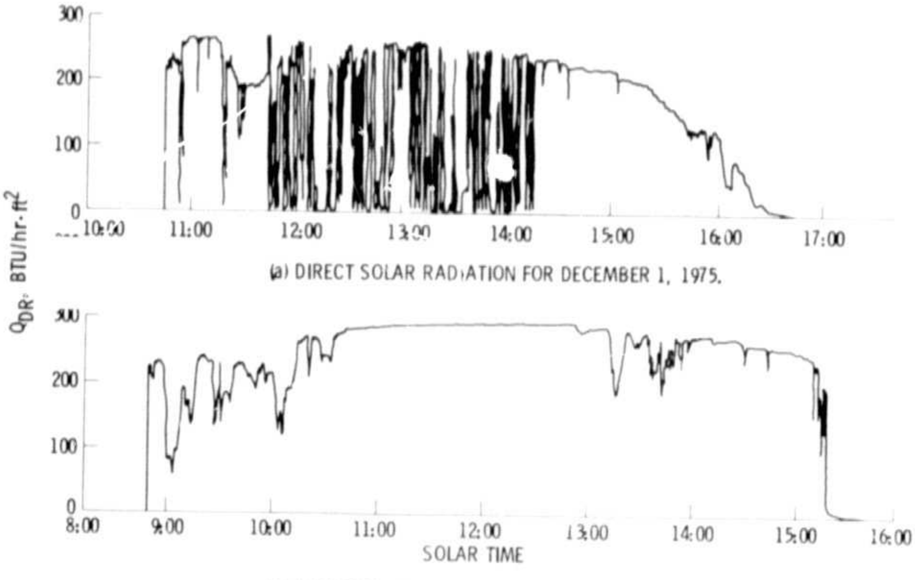

Figure 9. - Solar Radiation recorded from normal incidence pyrheliometer.